Original Article

The relationship between hematoma morphology and intraventricular hemorrhage in supratentorial deep intracerebral hemorrhage

Ying Li[1], Zhuangzhuang Zhang[1], Jieyu Li[1], Weiping Sun[1,2], Zhaoxia Wang[1,2], Yining Huang[1,2]

[1]Department of Neurology, Peking University First Hospital, Beijing, China; [2]Beijing Key Laboratory of Neurovascular Disease Discovery, Beijing, China

Contributions: (I) Conception and design: Y Li, W Sun; (II) Administrative support: W Sun, Z Wang, Y Huang; (III) Provision of study materials or patients: Y Li; (IV) Collection and assembly of data: Y Li, J Li; (V) Data analysis and interpretation: Y Li, Z Zhang; (VI) Manuscript writing: All authors; (VII) Final approval of manuscript: All authors.

Correspondence to: Weiping Sun, MD, MHSc; Zhaoxia Wang, MD. Beijing Key Laboratory of Neurovascular Disease Discovery, Beijing, China; Department of Neurology, Peking University First Hospital, 8 Xishiku Street, Beijing 100034, China. Email: sunweiping1979@163.com; drwangzx@163.com.

Background: Intraventricular hemorrhage (IVH) after intracerebral hemorrhage (ICH) is a strong independent predictor of poor outcomes. Although the location and volume of ICH are associated with IVH, our knowledge concerning the mechanism of IVH after ICH is still limited. This study aimed to investigate the relationship between hematoma morphology and IVH in patients with supratentorial deep ICH.

Methods: We retrospectively analyzed adult patients (aged ≥18 years) with spontaneous supratentorial deep ICH who underwent computed tomography (CT) within 48 h after ICH symptom onset in Peking University First Hospital between January 2017 and August 2022. We collected the clinical and imaging data of the patients and assessed hematoma morphology using several quantitative radiological parameters including hematoma volume, sphericity index, A/B ratio (A: the largest area of hematoma; B: the largest diameter 90° to A on the same slice), and our newly proposed largest diameter-midline angle (LMA). Multivariable logistic regression analysis was used to analyze the relationship between these parameters and the presence of IVH on the initial CT scan.

Results: Among 114 patients with spontaneous supratentorial deep ICH, 41 (36.0%) had IVH. In patients with IVH, the sphericity index was lower than that in individuals without IVH, while the LMA was larger. Multivariate logistic regression analysis showed that sphericity index [0.1-unit odds ratio (OR) =0.252; 95% CI: 0.089–0.709; P=0.009] and the LMA (10-unit OR =1.281; 95% CI: 1.007–1.630; P=0.04) were independently associated with the presence of IVH in patients with supratentorial deep ICH. Univariate analyses showed that hematoma volume, A/B ratio, sphericity index, and the LMA were significantly associated with poor outcomes at discharge.

Conclusions: Two quantitative parameters of hematoma morphology, sphericity index and the LMA, were significantly associated with the presence of IVH in patients with supratentorial deep ICH. Further prospective studies with larger sample sizes are needed to validate our results.

Keywords: Intracerebral hemorrhage (ICH); intraventricular hemorrhage (IVH); hematoma morphology; three-dimensional (3D); risk factor

Submitted Mar 03, 2023. Accepted for publication Aug 06, 2023. Published online Sep 18, 2023.
doi: 10.21037/qims-23-266
View this article at: https://dx.doi.org/10.21037/qims-23-266

Introduction

Spontaneous intracerebral hemorrhage (ICH) is the least treatable form of stroke, has a high mortality rate, and accounts for approximately 10–30% of all strokes worldwide (1). Intraventricular hemorrhage (IVH), which occurs in 30–50% of patients with spontaneous ICH, is a strong independent predictor of poor outcomes, increasing mortality by up to 80% (2-6). Understanding the risk factors and pathophysiology of IVH may help to identify optimal therapeutic strategies. Multiple risk factors contributing to IVH after ICH, including the location and volume of hematoma, baseline arterial pressure, and moderate to severe white matter lesions, have been identified (4-9). Compared with lobar ICH, deep ICH involves an anatomical juxtaposition with the ventricles which makes them highly prevalent areas of IVH. A greater volume of hematoma evidently results in an extension into the ventricles because the ventricular system provides an outlet for hematoma expansion with less resistance than the brain parenchyma (4-7).

Prior studies have suggested that morphological features of hematoma, such as margin irregularity, are associated with hematoma expansion (10,11), but few studies have analyzed the relationship between hematoma morphology and IVH. Therefore, the objective of this study was to explore the association of quantitative parameters of hematoma morphology and the presence of IVH with the initial computed tomography (CT) scan of the patients with spontaneous supratentorial deep ICH. To this end, we used hematoma segmentation software that can provide three-dimensional (3D) volumetry and quantification. We present this article in accordance with the STROBE reporting checklist (available at https://qims.amegroups.com/article/view/10.21037/qims-23-266/rc).

Methods

Study patients

We conducted a retrospective review of a consecutive cohort of patients with ICH admitted to Peking University First Hospital between January 2017 and August 2022. Patients were included if they met the following criteria: (I) age ≥18 years; (II) spontaneous supratentorial deep ICH including the thalamus, globus pallidus, putamen, caudate head, and anterior and posterior limbs of the internal capsules; and (III) baseline noncontrast cranial CT obtained within 48 h of symptom onset. We excluded secondary hemorrhage due to other etiologies, such as aneurysm, vascular malformation, tumor, head trauma, venous infarction, or hemorrhagic transformation of ischemic infarction. We also excluded those patients with isolated IVH. Considering an association of ICH and chronic kidney disease and chronic liver disease, we excluded any patients with these comorbidities, the diagnosis of which was apparent in their medical history (12,13). This study was conducted in accordance with the Declaration of Helsinki (as revised in 2013) and was approved by the Ethics Committee of Peking University First Hospital (No. 2022-743). Individual consent for this retrospective analysis was waived.

Clinical data collection

Clinical data were abstracted from medical records, including demographics (age and sex), medical history (hypertension, diabetes mellitus, previous stroke, use of antiplatelet agents or anticoagulants within 72 h of onset), admission Glasgow Coma Scale (GCS) score, admission systolic blood pressure (SBP), admission diastolic blood pressure (DBP), admission glucose level, time to initial CT, and the modified Rankin Scale (mRS) score at discharge.

Imaging analysis

All CT images were acquired using a standard scanning parameter of 5-mm-thick slices (GE HealthCare, Chicago, IL, USA). The presence of IVH and parenchymal hematoma location were assessed based on the initial CT images. For further quantitative measurement, the CT scans were then postprocessed using 3D-Slicer 4.11 (http://www.slicer.org), an open-source medical image computing platform. Hematoma was automatically identified pixel by pixel in each slice after the thresholds were set at a range of 50 to 100 Hounsfield units (HU). Then a 3D model was constructed, and the volume and surface area were automatically computed (14) (*Figure 1*).

To assess the irregularity of the hematoma shape, we used the following sphericity definition as a shape irregularity index (15):

$$\text{Sphericity Index}(\text{SI}) = \frac{\pi^{1/3}(6\text{V})^{2/3}}{\text{Area}} \quad [1]$$

where "V" represents the volume (in cubic centimeters) and "Area" represents the surface area (in square centimeters) of the hematoma. The SI quantifies the irregularity of the

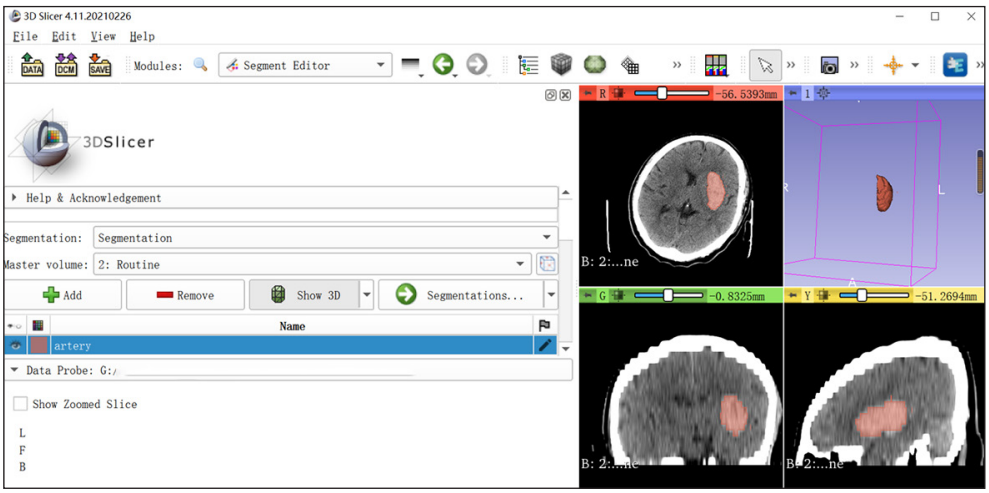

Figure 1 The hematoma model reconstructed using 3D-Slicer software. 3D, three-dimensional.

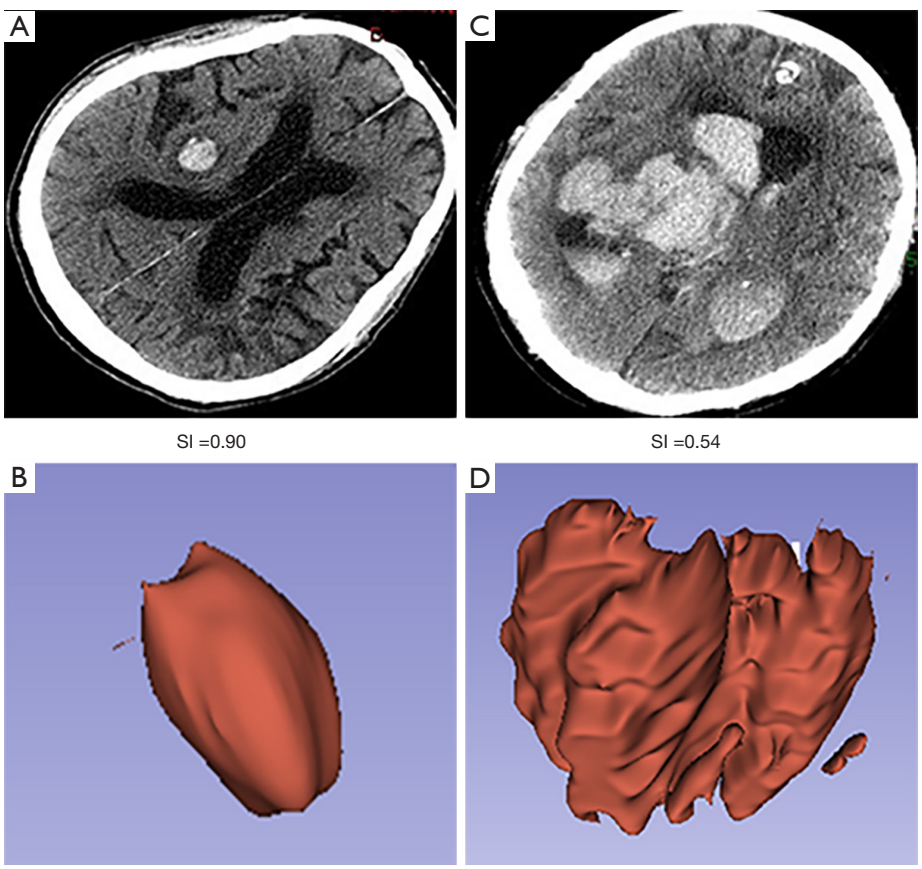

Figure 2 Axial CT images and 3D models with corresponding SI values of 2 patients with ICH. (A,B) Axial CT image and 3D model of a patient with ICH and a regular hematoma shape. (C,D) Axial CT image and 3D model of a patient with ICH and an irregular hematoma shape. 3D, three-dimensional; CT, computed tomography; SI, sphericity index; ICH, intracerebral hemorrhage.

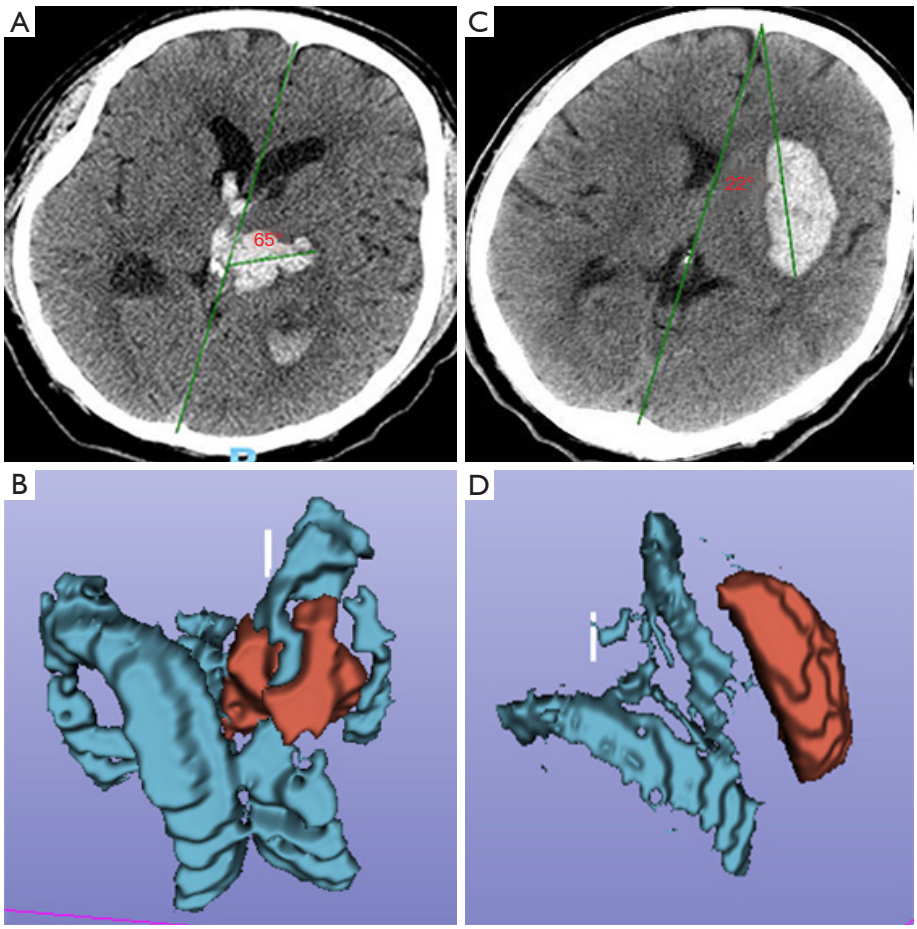

Figure 3 The LMA and 3D model of 2 patients with ICH. The LMA angle is the acute angle formed by the largest diameter of the hematoma and the midline of brain on the slice with the largest area of hematoma. (A,B) The LMA and 3D model of a patient with thalamic ICH. (C,D) The LMA and 3D model of a patient with putaminal ICH. The red area is the hematoma, and the blue area is the ventricular system. LMA, largest diameter-midline angle; 3D, three-dimensional; ICH, intracerebral hemorrhage.

hematoma shape from a range of 0 (very irregular surface) to 1 (perfectly regular surface) on a continuous scale (*Figure 2*) (16,17).

We measured the largest diameter on the CT slice with the largest area of hematoma (A) and the largest diameter 90° to A on the same slice (B), as mentioned in the classic ABC/2 method (18). We calculated the A/B ratio to assess the shape of the hematoma.

To describe the relative location of hematoma and ventricles, we measured the acute angle formed by the largest diameter of the hematoma and the midline of brain on the slice with the largest area of hematoma, which we termed the largest diameter-midline angle (LMA). As shown in *Figure 3*, a large LMA indicates that the hematoma is nearly perpendicular to the ventricles, while a small LMA indicates that the hematoma is nearly parallel to the ventricles.

Two experienced neurologists assessed all the images independently. The intraclass correlation coefficient (ICC) of the hematoma volume, SI, LMA, and A/B ratio were 0.991 (P<0.001), 0.969 (P<0.001), 0.796 (P<0.001), and 0.711 (P<0.001), respectively. The average values of these parameters were used in the subsequent analyses. With regard to the categorical variables such as hematoma location and the presence of IVH, a joint decision of both reviewers was made in cases of disagreement.

Statistical analysis

Continuous variables are expressed as mean± standard

deviation (SD) or median and interquartile range (IQR). Categorical variables are presented as frequencies with percentages. The demographic, clinical, and radiological characteristics were compared between patients with IVH and those without IVH using the chi-squared test, Fisher exact test, Student's *t*-test, or Mann-Whitney test as appropriate. The relationship between the quantitative parameters of hematoma morphology and the presence of IVH was assessed with univariate and multivariate logistic regression models. In the multivariable analyses, model 1 was adjusted for age and sex while model 2 was adjusted for age, sex, medical history (hypertension, diabetes mellitus, previous stroke, use of antiplatelet agents or anticoagulants within 72 h of onset), admission SBP, admission DBP, admission glucose, time to initial CT, and thalamic involvement. The association of the quantitative parameters of hematoma morphology and poor outcome at discharge was assessed using a univariate logistic regression analysis. Poor outcome was defined as an mRS score of 3–5 or death. For all statistical analyses, statistical significance was set at $P<0.05$. All statistical analyses were conducted using SPSS version 23.0 (IBM Corp., Armonk, NY, USA).

Results

Baseline characteristics

In total, 114 patients with spontaneous supratentorial deep ICH were included in the study. Of these, the hematoma was located in the thalamus in 50 (43.9%) patients, the lenticular nucleus in 49 (43.0%), the internal capsule in 11 (9.6%), and the caudate nucleus in 4 (3.5%). Moreover, 41 patients (36.0%) had IVH on the initial CT scan. The baseline clinical and radiological characteristics of the patients with and without IVH are shown in *Table 1*. In brief, a higher proportion of patients with severe ICH (GCS score 3–8) and thalamic involvement and higher admission glucose level were observed in the IVH group. The median hematoma volume was 8.0 mL (IQR, 5.6–14.6 mL) in patients with IVH compared to 4.3 mL (IQR, 1.5–11.9 mL) in patients without IVH. Compared with patients without IVH, those with IVH had a lower SI and A/B ratio and a larger LMA.

Association of the quantitative parameters of hematoma morphology and IVH

Table 2 details the association of the quantitative parameters of hematoma morphology and the presence of IVH. Lower SI and larger LMA were significantly associated with IVH in the unadjusted model. After adjustments were made for age, sex, and other confounding variables, SI [0.1-unit odds ratio (OR) =0.252; 95% CI: 0.089–0.709; P=0.009] and LMA (10-unit OR =1.281; 95% CI: 1.007–1.630; P=0.04) were still independently associated with IVH. There was no significant association between hematoma volume, A/B ratio, or IVH in the multivariable analyses.

Association of the quantitative parameters of hematoma morphology and poor outcome at discharge

There were 60 patients (52.6%) who had a poor outcome at discharge. Univariate analysis showed that hematoma volume (OR =1.162; 95% CI: 1.079–1.251), SI (OR =0.359; 95% CI: 0.209–0.616), A/B ratio (OR =0.290; 95% CI: 0.121–0.693), and LMA (OR =1.141; 95% CI: 1.003–1.298) were significantly associated with poor outcome at discharge.

Discussion

In this study, we found that SI and LMA, 2 parameters used for the quantitative evaluation of hematoma morphology, were independently associated with the presence of IVH in patients with supratentorial deep ICH. Patients with a lower SI and a larger LMA may thus be at a higher risk of IVH.

IVH is widely acknowledged to be an important predictor of poor outcome in ICH, with multiple pathophysiological mechanisms involved. The development of hydrocephalus is generally considered to be the most severe consequence of IVH (1,2). However, other studies have reported that in patients with IVH without obstructive hydrocephalus, the extent of IVH is still associated with clinical outcome, which suggests the involvement of other mechanisms besides the disturbance of cerebrospinal fluid circulation, such as the impairment of ependymal and subependymal structures and inflammatory intraventricular processes (19,20).

However, the mechanisms underlying the process by which parenchymal hematoma enters the ventricular system are much less well understood. Some studies have indicated that hematoma location and volume, along with arterial blood pressure fluctuation,are associated with hematoma extension into the ventricles (4-7). However, there is limited information concerning the relation between hematoma shape and IVH. Our data showed that SI, which quantitatively indicates the irregularity of the hematoma

Table 1 Baseline characteristics of study participants

Variables	Total (n=114)	With IVH (n=41)	Without IVH (n=73)	P value
Demographic factor				
Age, year	65.1 (13.6)	66.6 (13.5)	64.2 (13.7)	0.37
Female	31 (27.2)	14 (34.1)	17 (23.3)	0.21
Medical history				
Hypertension	97 (85.1)	35 (85.4)	62 (84.9)	0.95
Diabetes mellitus	27 (23.7)	12 (29.3)	15 (20.5)	0.29
Previous stroke	31 (27.2)	13 (31.7)	18 (24.7)	0.42
Antiplatelet use (n=112)	18 (16.1)	6 (14.6)	12 (16.9)	0.75
Anticoagulant use (n=112)	6 (5.4)	4 (9.8)	2 (2.8)	0.19
Clinical and laboratory features				
Admission GCS score (n=101)				0.03
9–15	90 (89.1)	25 (78.1)	65 (94.2)	
3–8	11 (10.9)	7 (21.9)	4 (5.8)	
Admission SBP, mmHg (n=96)	175.0 (160.0–198.5)	175.0 (164.0–189.5)	175.0 (153.0–203.0)	0.95
Admission DBP, mmHg (n=96)	99.5 (82.0–111.0)	92.0 (80.0–110.5)	100.0 (84.0–111.0)	0.29
Admission glucose, mmol/L (n=107)	7.2 (6.1–8.8)	7.5 (6.6–9.5)	6.8 (5.9–8.6)	0.02
Radiological features				
Time to initial CT, hours	3.0 (1.0–10.3)	3.0 (1.0–5.5)	3.0 (1.0–24.0)	0.16
Hematoma volume, mL	6.0 (2.6–13.3)	8.0 (5.6–14.6)	4.3 (1.5–11.9)	0.003
Thalamic involvement	52 (45.6)	27 (65.9)	25 (34.2)	0.001
SI	0.72 (0.09)	0.69 (0.09)	0.74 (0.08)	<0.001
A/B ratio[†]	1.5 (1.3–2.0)	1.5 (1.2–1.8)	1.7 (1.3–2.1)	0.04
LMA, °	37.5 (12.0–70.3)	60.0 (32.5–78.0)	22.0 (10.0–65.0)	<0.001

Values are reported as n (%), mean (SD), or median (IQR). [†], A: the largest area of hematoma; B: the largest diameter 90° to A on the same slice. IVH, intraventricular hemorrhage; GCS, Glasgow Coma Scale; SBP, systolic blood pressure; DBP, diastolic blood pressure; CT, computed tomography; SI, sphericity index; LMA, largest diameter-midline angle.

Table 2 Association of hematoma morphology and intraventricular hemorrhage

Variable	Unadjusted			Model 1			Model 2		
	OR	95% CI	P value	OR	95% CI	P value	OR	95% CI	P value
Hematoma volume	1.021	0.990–1.053	0.19	1.001	0.959–1.044	0.98	0.986	0.923–1.054	0.69
SI (per 0.1)	0.432	0.261–0.715	0.001	0.353	0.186–0.671	0.001	0.252	0.089–0.709	0.009
A/B ratio[†]	0.436	0.179–1.062	0.07	0.792	0.267–2.346	0.67	0.558	0.105–2.978	0.50
LMA (per 10°)	1.281	1.112–1.476	0.001	1.338	1.120–1.598	0.001	1.281	1.007–1.630	0.04

[†], A: the largest area of hematoma; B: the largest diameter 90° to A on the same slice. Model 1: adjusted for age and sex. Model 2: adjusted for age, sex, medical history (hypertension, diabetes mellitus, previous stroke, use of antiplatelet agents or anticoagulants within 72 h of onset), admission systolic blood pressure, admission diastolic blood pressure, admission glucose, time to initial CT, and thalamic involvement. OR, odds ratio; CI, confidence interval; SI, sphericity index; LMA, largest diameter-midline angle; CT, computed tomography.

shape, was associated with IVH. In previous reports, several authors categorized the shape of the hematoma into round and irregular (21-23), and the most commonly used method of classification was the 5-point categorical scale proposed by Barras *et al.* (24). As the shape of the hematoma is extremely variable, the simple categorical scale is neither as objective nor as accurate as is SI. Prior studies have demonstrated that the irregularity of hematoma shape is closely associated with hematoma expansion (10,11,25-27), and margin irregularity may reflect multiple origins or bleeding sources within the hematoma, which would be more likely to progress along multiple tracks and manifest as an irregular edge (10,24). Therefore, we speculated that the association between SI and IVH is potentially mediated by hematoma expansion.

We propose a novel parameter, LMA, to describe the relative position of supratentorial deep hematoma and ventricles. Interestingly, we found that LMA was associated with IVH. ICH is often considered to be a dynamic process rather than a static event (10,11,26-30). Hematoma growth occurs in a nonuniform pattern (31,32), and the largest diameter represents the main direction and trend of hematoma development. In addition, we reconstructed a 3D model of the hematoma and ventricles, which showed the anatomical relationship between them more intuitively. The presence of a larger LMA may suggest that the hematoma is oriented toward the ventricles and can easily break into the ventricles, which may explain the association between LMA and IVH. Previous research points to ICH volume as a risk factor of IVH (4). In our study, the patients with IVH had a larger hematoma volume than those without IVH. However, this difference became statistically nonsignificant after adjustments were made for confounders, which may be due to the fact that we only included those patients with supratentorial deep ICH and excluded those with lobar ICH and larger hematoma volume. However, owing to the small sample size of this study, further confirmation is required.

Our study found an association of the 4 parameters of hematoma morphology and poor outcome at discharge, supporting their potential value for predicting ICH outcome. However, as a retrospective study, patients' outcome was measured at discharge, and a small sample size limited the application of multivariable analysis. The relationship between hematoma morphology and ICH prognosis warrants further study.

As IVH was an independent predictor of poor outcome after ICH, our study found an association between the irregularity of hematoma shape and the relative position of hematoma and ventricles with IVH, a fact which may aid in screening those ICH patients with a high risk of poor outcome. Additionally, these findings may improve our understanding of the development of IVH and provide insights into the potential mechanism of IVH. Our work also reinforces the merit of quantitative evaluation based on a 3D reconstruction model in the study of IVH.

Our study had several limitations. First, although we found an association between hematoma shape and IVH on the initial CT scan, we employed a retrospective design, and thus the temporal relation between hematoma shape and IVH could not be established. Therefore, further prospective study is needed to clarify their relationship. Second, our study was performed in a single center with a small sample size; however, this dataset was homogeneous with regard to the study protocol. Furthermore, we excluded patients with lobar ICH, which limits the generalizability of our results. Third, a previous study reported that the risk factors of IVH after ICH include the location and volume of hematoma, baseline arterial pressure, and moderate-to-severe white matter lesions (4-9). In our study, the multivariate analysis indicated that SI and LMA were significantly associated with IVH after adjustments were made for age, hematoma location, and baseline arterial pressure. However, we used a cross-sectional analysis and thus cannot establish a temporal relationship. Further studies are needed to assess the predictive value of the radiological parameters of hematoma and compare them with the currently employed predictors.

Conclusions

SI and LMA, 2 parameters of hematoma morphology, were found to be independent risk factors of IVH in patients with supratentorial deep ICH. Due to the retrospective nature of our study design, further prospective research with larger sample sizes is needed to validate our results.

Acknowledgments

Funding: This work was supported by the National Natural Science Foundation of China (No. 81400944) and the Interdisciplinary Clinical Research Project of Peking University First Hospital (No. 2021CR37).

Footnote

Reporting Checklist: The authors have completed the

STROBE reporting checklist. Available at https://qims.amegroups.com/article/view/10.21037/qims-23-266/rc

Conflicts of Interest: All authors have completed the ICMJE uniform disclosure form (available at https://qims.amegroups.com/article/view/10.21037/qims-23-266/coif). The authors have no conflicts of interest to declare.

Ethical Statement: The authors are accountable for all aspects of the work in ensuring that questions related to the accuracy or integrity of any part of the work are appropriately investigated and resolved. This study was conducted in accordance with the Declaration of Helsinki (as revised in 2013) and was approved by the Ethics Committee of Peking University First Hospital (No. 2022-743). Individual consent for this retrospective analysis was waived.

References

1. Qureshi AI, Mendelow AD, Hanley DF. Intracerebral haemorrhage. Lancet 2009;373:1632-44.
2. Balami JS, Buchan AM. Complications of intracerebral haemorrhage. Lancet Neurol 2012;11:101-18.
3. Hanley DF. Intraventricular hemorrhage: severity factor and treatment target in spontaneous intracerebral hemorrhage. Stroke 2009;40:1533-8.
4. Steiner T, Diringer MN, Schneider D, Mayer SA, Begtrup K, Broderick J, Skolnick BE, Davis SM. Dynamics of intraventricular hemorrhage in patients with spontaneous intracerebral hemorrhage: risk factors, clinical impact, and effect of hemostatic therapy with recombinant activated factor VII. Neurosurgery 2006;59:767-73; discussion 773-4.
5. Bhattathiri PS, Gregson B, Prasad KS, Mendelow AD; STICH Investigators. Intraventricular hemorrhage and hydrocephalus after spontaneous intracerebral hemorrhage: results from the STICH trial. Acta Neurochir Suppl 2006;96:65-8.
6. Xie Y, Chen F, Li H, Wu Y, Fu H, Zhong Q, Chen J, Wang X. Development and validation of a clinical-radiomics nomogram for predicting a poor outcome and 30-day mortality after a spontaneous intracerebral hemorrhage. Quant Imaging Med Surg 2022;12:4900-13.
7. Tuhrim S, Horowitz DR, Sacher M, Godbold JH. Volume of ventricular blood is an important determinant of outcome in supratentorial intracerebral hemorrhage. Crit Care Med 1999;27:617-21.
8. Kim BJ, Lee SH, Ryu WS, Kim CK, Chung JW, Kim D, Park HK, Yoon BW. Extents of white matter lesions and increased intraventricular extension of intracerebral hemorrhage. Crit Care Med 2013;41:1325-31.
9. Vagal V, Venema SU, Behymer TP, Mistry EA, Sekar P, Sawyer RP, Gilkerson L, Moomaw CJ, Haverbusch M, Coleman ER, Flaherty ML, Van Sanford C, Stanton RJ, Anderson C, Rosand J, Woo D. White Matter Lesion Severity is Associated with Intraventricular Hemorrhage in Spontaneous Intracerebral Hemorrhage. J Stroke Cerebrovasc Dis 2020;29:104661.
10. Blacquiere D, Demchuk AM, Al-Hazzaa M, Deshpande A, Petrcich W, Aviv RI, et al. Intracerebral Hematoma Morphologic Appearance on Noncontrast Computed Tomography Predicts Significant Hematoma Expansion. Stroke 2015;46:3111-6.
11. Morotti A, Boulouis G, Romero JM, Brouwers HB, Jessel MJ, Vashkevich A, Schwab K, Afzal MR, Cassarly C, Greenberg SM, Martin RH, Qureshi AI, Rosand J, Goldstein JN; . Blood pressure reduction and noncontrast CT markers of intracerebral hemorrhage expansion. Neurology 2017;89:548-54.
12. Vanent KN, Leasure AC, Acosta JN, Kuohn LR, Woo D, Murthy SB, Kamel H, Messé SR, Mullen MT, Cohen JB, Cohen DL, Townsend RR, Petersen NH, Sansing LH, Gill TM, Sheth KN, Falcone GJ. Association of Chronic Kidney Disease With Risk of Intracerebral Hemorrhage. JAMA Neurol 2022;79:911-8.
13. Hoya K, Tanaka Y, Uchida T, Takano I, Nagaishi M, Kowata K, Hyodo A. Intracerebral hemorrhage in patients with chronic liver disease. Neurol Med Chir (Tokyo) 2012;52:181-5.
14. Xu X, Chen X, Zhang J, Zheng Y, Sun G, Yu X, Xu B. Comparison of the Tada formula with software slicer: precise and low-cost method for volume assessment of intracerebral hematoma. Stroke 2014;45:3433-5.
15. Salazar P, Di Napoli M, Jafari M, Jafarli A, Ziai W, Petersen A, Mayer SA, Bershad EM, Damani R, Divani AA. Exploration of Multiparameter Hematoma 3D Image

Analysis for Predicting Outcome After Intracerebral Hemorrhage. Neurocrit Care 2020;32:539-49.
16. Poplawski NJ, Shirinifard A, Agero U, Gens JS, Swat M, Glazier JA. Front instabilities and invasiveness of simulated 3D avascular tumors. PLoS One 2010;5:e10641.
17. Lee JH, Park CM, Park SJ, Bae JS, Lee SM, Goo JM. Value of Computerized 3D Shape Analysis in Differentiating Encapsulated from Invasive Thymomas. PLoS One 2015;10:e0126175.
18. Kothari RU, Brott T, Broderick JP, Barsan WG, Sauerbeck LR, Zuccarello M, Khoury J. The ABCs of measuring intracerebral hemorrhage volumes. Stroke 1996;27:1304-5.
19. Hwang BY, Bruce SS, Appelboom G, Piazza MA, Carpenter AM, Gigante PR, Kellner CP, Ducruet AF, Kellner MA, Deb-Sen R, Vaughan KA, Meyers PM, Connolly ES Jr. Evaluation of intraventricular hemorrhage assessment methods for predicting outcome following intracerebral hemorrhage. J Neurosurg 2012;116:185-92.
20. Kumar V, Umair Z, Kumar S, Goutam RS, Park S, Kim J. The regulatory roles of motile cilia in CSF circulation and hydrocephalus. Fluids Barriers CNS 2021;18:31.
21. Fujii Y, Tanaka R, Takeuchi S, Koike T, Minakawa T, Sasaki O. Hematoma enlargement in spontaneous intracerebral hemorrhage. J Neurosurg 1994;80:51-7.
22. Zhan RY, Tong Y, Shen JF, Lang E, Preul C, Hempelmann RG, Hugo HH, Buhl R, Barth H, Klinge H, Mehdorn HM. Study of clinical features of amyloid angiopathy hemorrhage and hypertensive intracerebral hemorrhage. J Zhejiang Univ Sci 2004;5:1262-9.
23. Huttner HB, Steiner T, Hartmann M, Köhrmann M, Juettler E, Mueller S, Wikner J, Meyding-Lamade U, Schramm P, Schwab S, Schellinger PD. Comparison of ABC/2 estimation technique to computer-assisted planimetric analysis in warfarin-related intracerebral parenchymal hemorrhage. Stroke 2006;37:404-8.
24. Barras CD, Tress BM, Christensen S, MacGregor L, Collins M, Desmond PM, Skolnick BE, Mayer SA, Broderick JP, Diringer MN, Steiner T, Davis SM; . Density and shape as CT predictors of intracerebral hemorrhage growth. Stroke 2009;40:1325-31.
25. Morotti A, Boulouis G, Dowlatshahi D, Li Q, Shamy M, Al-Shahi Salman R, Rosand J, Cordonnier C, Goldstein JN, Charidimou A. Intracerebral haemorrhage expansion: definitions, predictors, and prevention. Lancet Neurol 2023;22:159-71.
26. Boulouis G, Morotti A, Brouwers HB, Charidimou A, Jessel MJ, Auriel E, Pontes-Neto O, Ayres A, Vashkevich A, Schwab KM, Rosand J, Viswanathan A, Gurol ME, Greenberg SM, Goldstein JN. Association Between Hypodensities Detected by Computed Tomography and Hematoma Expansion in Patients With Intracerebral Hemorrhage. JAMA Neurol 2016;73:961-8.
27. Elkhatib THM, Shehta N, Bessar AA. Hematoma Expansion Predictors: Laboratory and Radiological Risk Factors in Patients with Acute Intracerebral Hemorrhage: A Prospective Observational Study. J Stroke Cerebrovasc Dis 2019;28:2177-86.
28. Takeda R, Ogura T, Ooigawa H, Fushihara G, Yoshikawa S, Okada D, Araki R, Kurita H. A practical prediction model for early hematoma expansion in spontaneous deep ganglionic intracerebral hemorrhage. Clin Neurol Neurosurg 2013;115:1028-31.
29. Yao X, Xu Y, Siwila-Sackman E, Wu B, Selim M. The HEP Score: A Nomogram-Derived Hematoma Expansion Prediction Scale. Neurocrit Care 2015;23:179-87.
30. Ji N, Lu JJ, Zhao YL, Wang S, Zhao JZ. Imaging and clinical prognostic indicators for early hematoma enlargement after spontaneous intracerebral hemorrhage. Neurol Res 2009;31:362-6.
31. Boulouis G, Dumas A, Betensky RA, Brouwers HB, Fotiadis P, Vashkevich A, Ayres A, Schwab K, Romero JM, Smith EE, Viswanathan A, Goldstein JN, Rosand J, Gurol ME, Greenberg SM. Anatomic pattern of intracerebral hemorrhage expansion: relation to CT angiography spot sign and hematoma center. Stroke 2014;45:1154-6.
32. Liu R, Huynh TJ, Huang Y, Ramsay D, Hynynen K, Aviv RI. Modeling the pattern of contrast extravasation in acute intracerebral hemorrhage using dynamic contrast-enhanced MR. Neurocrit Care 2015;22:320-4.

Cite this article as: Li Y, Zhang Z, Li J, Sun W, Wang Z, Huang Y. The relationship between hematoma morphology and intraventricular hemorrhage in supratentorial deep intracerebral hemorrhage. Quant Imaging Med Surg 2023;13(10):6854-6862. doi: 10.21037/qims-23-266

